GEOPHYSICAL RESEARCH LETTERS, VOL. 24, NO. 16, PAGES 2031-2034, AUGUST 15, 1997

El Niño: A coupled response to radiative heating?

De-Zheng Sun

NOAA-CIRES/Climate Diagnostics Center, Boulder, CO

Abstract. The very existence of El Niño – the oscillatory behavior of the tropical Pacific climate – may be due to the warmth of the tropics (relative to the coldness of the high latitudes). This is elucidated by subjecting a mathematical model for the coupled tropical ocean-atmosphere system to a varying radiative heating. The temperature of the deep ocean is kept fixed. In response to an increasing radiative heating, the coupled system first experiences a pitch-fork bifurcation that breaks the zonal symmetry imposed by the solar radiation. The resulting zonal sea surface temperature (SST) gradients increase with increases in the radiative heating. When the zonal SST gradients exceed a critical value, a Hopf bifurcation takes place which brings the system to an oscillatory state, a state that closely resembles the observed tropical Pacific climate. Further increases in the radiative heating result in increases in the magnitude of the oscillation. The results shed new light on the physics of El Niño and suggest that climate change due to anthropogenic forcing may occur through the same dynamic modes that sustain natural variability.

Introduction

A prominent feature of the tropical Pacific climate is the El Niño-Southern Oscillation (ENSO), a phenomenon characterized by periodic weakening/strengthening of the zonal SST contrast (Philander 1990). Climatic fluctuations world-wide have been associated with ENSO (Rasmusson and Wallace 1983). Previous studies of ENSO have attributed the existence of ENSO to the interaction between the atmosphere and ocean (Bjerknes 1969, Zebiak and Cane 1987, Battisti 1988, Suarez and Schopf 1988, Neelin 1991, Jin 1996). Whether the existence of ENSO is in any important way related to the intensity of radiative heating is unclear. It is the purpose of this letter to elucidate that ENSO also results from the warmth of the tropics, or more accurately, from the dynamic tension between the warmth that the solar radiation and greenhouse effect attempt to create and the coldness that the subsurface ocean tries to retain. We will show that ocean-atmosphere interaction is a necessary, but not sufficient condition for the birth of El Niño.

Paper number 97GL01960
0094-8534/97/97GL-01960$05.00

The Model

Focusing on the two fundamental features of the tropical Pacific climate, the zonal SST contrast and ENSO, we may reduce the coupled ocean-atmosphere to a low-order system through spatial truncation (Neelin 1991, Sun and Liu 1996). The resulting model is schematically illustrated in Fig. 1. The model for the equatorial ocean is a shallow water model embedding a mixed layer with a fixed depth. Following Sun and Liu (1996), the surface ocean is divided into two regions with equal areas: the western surface ocean (120 E-155 W) and the eastern surface ocean (155W-70W). They are represented respectively by two boxes with temperature T_1 and T_2. The atmosphere is approximated by a linear feedback system whose surface winds are driven by SST gradients and whose thermal effect is to force the surface ocean to reach a thermodynamic equilibrium (Neelin 1991, Sun and Liu 1996).

With these approximations, the heat budget for the two surface boxes over time t may be written as

$$\frac{dT_1}{dt} = c(T_e - T_1) + sq(T_2 - T_1) \qquad (1)$$

$$\frac{dT_2}{dt} = c(T_e - T_2) + q(T_{sub} - T_2) \qquad (2)$$

The two terms on the right hand of Eqs. (1) and (2) represent respectively the effect of the local heat flux into the ocean and the effect of advection by ocean currents. T_e is the SST the ocean would attain in the absence of the ocean currents. Oceanic transport tends to cool the surface ocean and therefore T_e is the maximum SST the tropical ocean can attain. c is a constant that measures the efficiency of atmospheric processes in removing a basin-wide SST anomaly. The value of T_e is proportional to the greenhouse effect and the solar radiation (Sun and Liu 1996). $q = \frac{W}{H_1}$, where W is the upwelling velocity and H_1 is the depth of the mixed layer. Zonal flow is assumed to be a fraction of the total upwelling and this fraction is measured by s. The value of q is given by

$$q = \frac{\alpha}{a}(T_1 - T_2) \qquad (3)$$

where α measures the sensitivity of wind-stress to changes in the SST gradients, a defines the adjustment time scale of the ocean currents to surface winds. In deriving Eq. (3), we have assumed that the surface wind stress is proportional to the zonal SST gradients and that the strength of ocean currents is proportional to

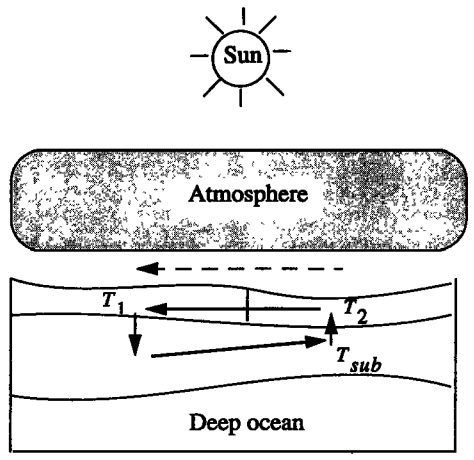

Figure 1. A schematic diagram for the coupled model. Solid arrows represent the zonal branch of the equatorial wind-driven circulation constituted by the upwelling in the east Pacific, the westward surface drift, and the equatorial undercurrent. The dashed arrow represents the surface winds.

the surface wind stress (Sun and Liu 1996). T_{sub} in Eq. (2) is the temperature of the water upwelled into the mixed layer. Using $\Phi(z)$ to represent the temperature profile of the subsurface upper ocean in the absence of winds and assuming that the effect of zonal variation of the upper ocean depth is simply to displace the profile $\Phi(z)$ vertically (Zebiak and Cane 1987) we have

$$T_{sub} = \Phi(-H_1 + h_2') \tag{4}$$

where h_2' is the deviation of the depth of the upper eastern Pacific ocean from its reference value H. H is the depth of the upper ocean when there are no winds. $\Phi(z)$ may be parameterized as follows,

$$\Phi(z) = T_e - \frac{T_e - T_b}{2}(1 - tanh(\frac{z + z_0}{H^*})) \tag{5}$$

where T_b is a reference temperature for defining the warmth of the tropics. H^* and z_0 are constants that have the unit of depth. T_b may be interpreted as the temperature of the equatorial deep ocean. The basic physics embodied in Eq. (5) is that the vertical temperature gradients in the equatorial ocean result from a competition between atmospheric heating from above and upwelling of cold water from below. The exponential form is based on observations (Zebiak and Cane 1987) and is also consistent with results from theoretical and numerical models of the thermocline (Verdiere 1988, Munk 1966). The variations of the depth of the upper ocean (or the thermocline) are governed by the following equations,

$$h_2' - h_1' = -\frac{H_1}{H_2} H \frac{\alpha}{b^2}(T_1 - T_2) \tag{6}$$

$$\frac{1}{r}\frac{dh_1'}{dt} = -h_1' + \frac{H_1}{2H_2} H \frac{\alpha}{b^2}(T_1 - T_2) \tag{7}$$

Eq. (6) represents the balance between the zonal pressure gradients and the zonal wind stress. h_1' is the deviation of the upper ocean depth in the western Pacific from its reference value H. $H_2 = H - H_1$. $b = \frac{c_k}{L_x}$ where c_k is the speed of the first baroclinic Kelvin wave and L_x is the half width of the basin. Eq. (7) is an approximate way to represent the slow adjustment of the thermocline depth to its equilibrium value determined by the surface wind-stress and mass conservation. r defines the time scale of this slow adjustment (or the memory of the upper ocean) (Jin 1996).

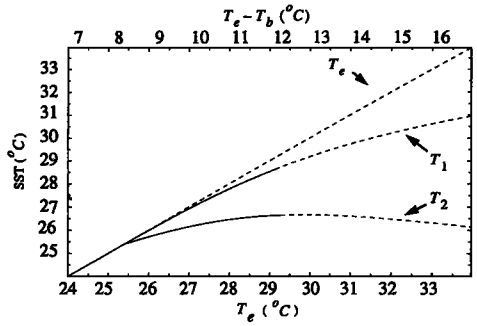

Figure 2. Equilibrium solutions of the coupled system as a function of T_e. The value for T_b is fixed at 17.3° C. The corresponding differences between T_e and T_b are also marked in the figure. Dashed lines indicate that the solution exists, but unstable. Parameters used are: $\frac{1}{c}$ = 150 days, $\frac{1}{r}$ = 300 days, $\frac{\alpha}{a} = 3.0 \times 10^{-8}\ K^{-1}s^{-1}$, $\frac{\rho\alpha}{b^2}H_2 = 11.5\ mK^{-1}$, H^* = 65 m, H_1 = 50 m, and z_0 = 75 m.

Equilibrium Solutions

Fig. 2 shows the equilibrium SST of the coupled system as a function of T_e. The value of T_e for the present climate is about $29.5°C$, as indicated by the observation that the heat flux into the warmest part of the tropical Pacific ocean is nearly zero (Ramanathan et al. 1995). Starting from a much colder T_e than the value for the observed climate, the coupled system has no zonal SST gradients. The SST increases linearly with increases in T_e. Zonal SST gradients are developed after T_e reaches $25.5°C$. The SST gradients increase quickly with further increases in T_e. The increases in the SST gradients are mainly due to increases in T_1. When T_e exceeds ap-

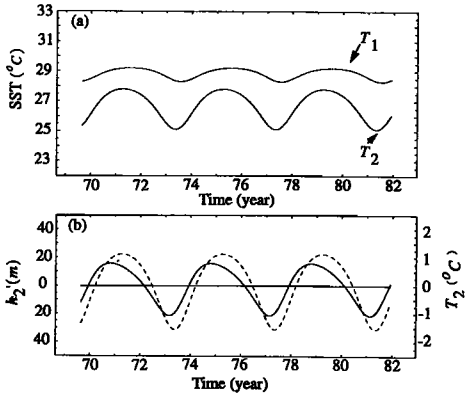

Figure 3. Oscillations at $T_e = 29.5°C$, a value corresponding to the observed climate. (a): variations of T_1 and T_2. (b): variations of h_2' (anomalies). The dashed line is anomalies of T_2.

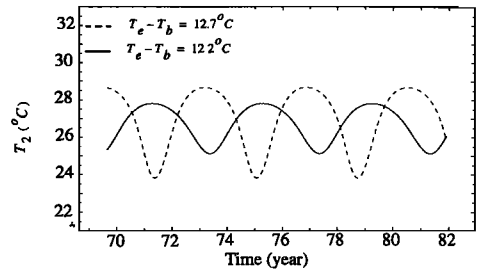

Figure 4. Oscillations of T_2 at $T_e = 29.5^o$ C (solid line) and $T_e = 30^o$ C (dashed line). The value for T_b is fixed at 17.3^o C. An increase in the magnitude of oscillation can also be created by reducing the value of T_b while keeping the value of T_e fixed.

proximately 29.2^oC, a Hopf bifurcation takes place and the coupled system starts to oscillate. Oscillations at $T_e = 29.5^oC$ are plotted in Fig. 3. The oscillations have a period of about 4 years with a slight westward phase tilt (Fig. 3a). The variations of the depth of the thermocline in the eastern half of the ocean also lead slightly the variations of SST in that region (Fig. 3b). All these features agree well with those of observed ENSO (Rasmusson and Carpenter 1982, Wang and Fang 1996). The zonal SST contrast at $T_e = 29.5^oC$ is somewhat smaller than observed. Further increases in T_e result in increases in the magnitude of the oscillation with relatively little change in the corresponding time mean (Fig. 4).

The Physics of ENSO

To understand the physics of the two bifurcations in Fig. 2, we replace (5) by a linear profile so that Eq. (4) can be written as,

$$T_{sub} = T_{s0} + \gamma h_2' \tag{8}$$

where $T_{s0} = \lambda T_e + (1-\lambda)T_b$ and $\gamma = \gamma^* \frac{T_e - T_{s0}}{H_2}$. λ and γ^* are numerical constants that are related to z_0 and H^* in Eq. (5). Eq. (8) may be regarded as a first order approximation of Eq. (5) with T_{s0} and γ being respectively the characteristic temperature and the lapse rate of the upper subsurface ocean. With Eq. (8) for T_{sub}, the coupled system has qualitatively the same behavior as shown in Fig. 2.

We non-dimensionalize Eqs. (1), (2), (3), (6), (7), and (8) by introducing $\tau = ct$, $q^* = \frac{q}{c}$, $T_1^* = \frac{T_1 - T_e}{T_e - T_{s0}}$, $T_2^* = \frac{T_2 - T_e}{T_e - T_{s0}}$, $T_{sub}^* = \frac{T_{sub} - T_e}{T_e - T_{s0}}$, $h_2'^* = \frac{h_2'}{H_2}$, and $h_1'^* = \frac{h_1'}{H_2}$. After non-dimensionalization, we find that the dynamic behavior of the system is determined by four non-dimensional parameters: $R = \frac{\alpha(T_e - T_{s0})}{ac}$, $\Lambda = p\kappa\gamma^*$ (where $p = \frac{H_1}{2H_2}(1 + \frac{H_1}{H_2})$ and $\kappa = \frac{ac}{b^2}$), $\delta = \frac{r}{c}$, and s.

The non-dimensional parameter R is analogous to the Rayleigh number in the classical problem of Rayleigh-Bénard convection (Rayleigh 1916). It measures how hard the system is driven, relative to the dissipation. In the present case, the driving force for the circulation is from the dynamic tension between the warmth that the greenhouse effect and the solar radiation tend to create (T_e) and the coolness that the subsurface ocean tries to retain (T_{s0}). The dissipation is from the mechanical and thermal damping. The thermal damping depends on the radiative feedbacks (Sun and Liu 1996). It is readily shown that the first bifurcation takes place when R=1. This is easy to understand because the driving force has to be strong enough to overcome dissipation in order to create and maintain a steady circulation.

The second bifurcation takes place when $R = R_c \simeq \frac{C}{\Lambda}$ where C is a parameter whose value depends only on the values of s and δ. For s=$\frac{1}{3}$, $\sigma = \frac{1}{2}$ (the values used in Fig. 2), C is about 1 (Fig. 5). C increases with increases in either s or δ. As long as $s \neq 0$, C remains a finite value even when the ocean has no memory (i.e., $r = \infty$ or $\delta = \infty$). For example, with s=$\frac{1}{3}$, C=1.5 for $\delta = \infty$. It is easy to show that $\frac{\partial T_{sub}}{\partial T_2} = \Lambda R$. Therefore, when the circulation in equilibrium is perturbed by a cooling in $T_2{}^*$ in the amount of $-\delta T_2$, the corresponding change in $T_{sub}{}^*$ will be $-\Lambda R \delta T_2{}^*$. A decrease in T_{sub} enhances the cooling effect of the upwelling upon T_2. When ΛR is sufficiently large, the enhanced cooling from the upwelling is able to overcome the opposing effect from the accompanying increase in the surface heat flux and consequently the initial cooling in T_2 will be further amplified. The instability is an oscillatory one because after some time, the decrease in T_{sub} is slowed down and eventually stopped by the adjustment of T_1 to changes in the cooling from the zonal advection and by the adjustment of h_1' to changes in the zonal SST contrast. The corresponding saturation and decrease in the cooling from the upwelling allows the surface heating to catch up to stop and eventually reverse the cooling in T_2. In short, critical for the instability of the steady circulation is that the temperature of the upwelled water depends strongly on the strength of the flow rate (i.e., a large Λ) and that the flow rate (or the thermal forcing that drives the flow) is sufficiently large relative to the thermal and mechanical damping (i.e., a large R). A similar mechanism is responsible for the onset of oscillation in the Lorenz system (Lorenz 1963) which is a low-order approximation of Rayleigh-Bénard convection. Thus, fundamentally, ENSO arises from an intensified competition between the warming effects from the atmosphere and the cooling effects from the subsurface ocean. Further intensification of this competition by increasing the differences between T_e and T_b results in

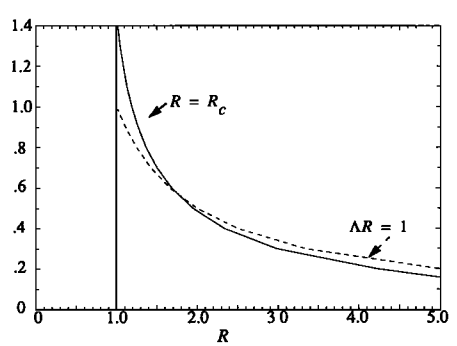

Figure 5. The critical value of R at which the Hopf bifurcation takes place as a function of Λ. $s = \frac{1}{3}$ and $\delta = \frac{1}{2}$. The dashed line is for $R = \frac{1}{\Lambda}$.

increases in the magnitude of the oscillation (Fig. 4). Note also that $\Lambda \sim b^{-2} = (\frac{L_x}{c_k})^2$. Therefore the critical value of R or T_e for the onset of oscillation ($\frac{C}{\Lambda}$) is inversely proportional to the width of the basin. This explains the absence of self-sustaining ENSO-like phenomena in the tropical Atlantic ocean whose width is only one third that of the tropical Pacific ocean.

Discussion

The non-dimensional analysis also reveals that it is the difference between T_e and T_b, not the absolute value of either of them that determines the strength of the zonal SST contrast and the magnitude of El Niño. This result raises an interesting prospect for the response of the tropical Pacific climate to an enhanced greenhouse effect which is that the response may depend on the time-scale of concern. Before the equatorial deep ocean feels the enhanced thermal forcing, the zonal SST contrast and the magnitude of ENSO will increase with increases in the greenhouse effect. When the temperature of the equatorial deep ocean equilibrates with the SST of the polar oceans, increases in T_b may eventually exceed the increases in T_e, and correspondingly the magnitude of ENSO may start to decrease. To address this interesting prospect rigorously is beyond the purpose of this letter which is mainly to illustrate that ENSO is a thermally forced oscillation. The reader can easily verify, however, that increasing the value of T_b by 1 ^oC or more while keeping T_e fixed to the value of 29.5^oC results in a tropical Pacific climate that has no El Niño. Correspondingly, when trying to understand why a particular past climate has no ENSO or a different SST contrast, one has to measure the warmth of the tropics relative to the coolness of the high latitudes. In the same vein, one possible explanation for the reduced zonal SST contrast and the absence of ENSO during the relatively warmer period of mid and early Holocene (Sandweiss et al. 1996) is that the temperature of the high latitudes increased more than the SST of the warm pool. For the same reason, we suspect that the reduced magnitude of ENSO found by Knutson and Manabe (1994) in their equilibrium runs of a global coupled model may be due to a reduced difference between T_e and T_b caused by the polar amplification of the global warming. The contradiction between the results from tropical upper ocean models (Clement et al 1996, Seager and Murtugudde 1997) and those from global ocean models on the equilibrium response of the zonal SST contrast to an increase in the radiative heating may also be reconciled by the present theoretical framework.

Of particular concern in the study of climate change is whether climate change due to anthropogenic enhancement of the greenhouse effect will take place through the same dynamic modes that sustain natural variability. The present findings suggest a positive answer to this question. The good news from this is that the bountiful observations of ENSO can be directly exploited to calculate climatic feedbacks and thereby the response of the tropical climate to anthropogenic forcing. The less encouraging news is that the anthropogenic change and natural variability may be much more convoluted in the Earth's climate record than a simple superposition of two independent signals.

Acknowledgments.
The author is grateful to Dr. P. Gent and Dr. F. Bryan for their advice on ocean dynamics. The author also wishes to thank Dr. D. Battisti, Dr. D. Neelin, Dr. R. Seager, and Dr. J. Tribbia for their helpful comments. This research was supported by NSF and NOAA.

References

Bjerknes, J., Atmospheric teleconnections from the equatorial Pacific, Mon. Wea. Rev., 97, 163-172, 1969.

Battisti, D. S., The dynamics and thermodynamics of a warm event in a coupled ocean-atmosphere model, J. Atmos. Sci., 45, 2889-2919, 1988.

Clement, A., R. Seager, M. A. Cane, and S. E. Zebiak, An ocean dynamical thermostat, J. Climate, 9, 2190-2196, 1996.

Jin, F. F., Tropical ocean-atmosphere interaction, the Pacific cold tongue, and the El Niño-Southern Oscillation, Science, 274, 76-78, 1996.

Knutson, T. R. and S. Manabe, Impact of increases CO_2 on simulated ENSO-like phenomena, Geophys. Res. Lett., 21, 2295-2298, 1994.

Lorenz, E., Deterministic nonperiodic flow, J. Atmos. Sci., 20, 131-141, 1963.

Munk, W. H., Abyssal recipes, Deep Sea Res., 13, 707-730, 1966.

Neelin, J.D., 1991: The slow sea surface temperature mode and the fast wave limit, J. Atmos. Sci., 48, 584-606, 1991.

Philander, S.G. *El Niño; La Niña, and the Southern Oscillation.* Academic Press, New York, 293 pp, 1990

Ramanathan, V., B. Subasilar, G. J. Zhang, W. Conant, R.D. Cess, J. T. Kiehl, H. Grassl, and L. Shi: Warm pool heat budget and shortwave cloud forcing: A missing physics. Science, 267, 499-503, 1995.

Rasmusson, E. M. and J. M. Wallace, Meteorological aspects of the El Niño/Southern Oscillation, Science, 222, 1195-1202, 1983.

Rasmusson, E. M. and T.H. Carpenter, Variations in tropical sea surface temperature and surface winds associated with the Southern Oscillation/El Niño, Mon. Wea. Rev., 110, 354-383, 1982.

Rayleigh, Lord, On convection currents in a horizontal layer of fluid when the higher temperature is on the under side, Phil. Mag., 32, 529-546, 1916.

Sandweiss et al., Geoarchaeological evidence from Peru for a 5000 years B.P. onset of El Niño, Science, 273, 1531-1533, 1996.

Seager, R. and R. Murtugudde, Ocean dynamics, thermocline adjustment and regulation of tropical SST, J. Climate, 10, 521-534, 1997.

Suarez, M. J. and P. Schopf, A delayed action oscillator for ENSO. J. Atmos. Sci., 45, 3283-3287, 1988.

Sun, D.Z. and Z. Liu, Dynamic ocean-atmosphere coupling, a thermostat for the tropics, Science, 272, 1148-1150, 1996.

Verdiere, A. C., Buoyancy driven planetary flow *J. Mar. Res.*, 46, 215-265, 1988.

Wang, B. and Z. Fang, Chaotic oscillations of tropical climate: a dynamic system theory for ENSO, J. Atmos. Sci., 53, 2786-2802, 1996.

Zebiak, S. E. and M. A. Cane, A model El Niño and Southern Oscillation, Mon. Wea. Rev., 115, 2262-2278, 1987.

NOAA-CIRES/CDC, CU/CIRES, Campus Box 449, Boulder, CO 80309. (e-mail: ds@cdc.noaa.gov)

(Received February 28, 1997; revised June 3, 1997; accepted June 20, 1997.)